Tetrahedron 64 (2008) 8307–8317

Contents lists available at ScienceDirect

Tetrahedron

journal homepage: www.elsevier.com/locate/tet

Reversibly controllable guest binding in precisely defined cavities: selectivity, induced fit, and switching in novel resorcin[4]arene-based container molecules

Thomas Gottschalk, Peter D. Jarowski, François Diederich *

Laboratorium für Organische Chemie, ETH Zürich, Hönggerberg, HCI, CH-8093 Zürich, Switzerland

ARTICLE INFO

Article history:
Received 19 February 2008
Received in revised form 4 April 2008
Accepted 25 April 2008
Available online 30 April 2008

Dedicated to Professor Sir J. Fraser Stoddart

Keywords:
Container molecules
Supramolecular chemistry
Molecular recognition
Controllable encapsulation
Molecular switches
Molecular dynamics

ABSTRACT

Two molecular baskets are presented, which were constructed based on a resorcin[4]arene platform. The molecules completely surround suitable guests, such as cyclo- or oxacycloalkanes, and bind them with high strength. The thermodynamic parameters for inclusion complexation were determined as well as the influence of encapsulation on the ring inversion barrier of bound cyclohexane. Two-dimensional NMR spectroscopy clearly shows the existence of a directed attractive interaction between oxacyclohexane and one of the hosts, which constrains the rotation of the bound molecule. Both containers exhibit remarkable binding selectivity as a consequence of their precisely defined structures. They both differentiate between homologous cycloalkanes, and whereas cyclohexane binds best within the larger of the two interior cavities, cyclopentane fits best in the smaller one. The selectivity is governed by ideal filling of space. We have conducted molecular dynamics experiments to understand the thermal fluctuations in the cavity sizes when a guest is bound. The simulations show that within a very narrow range the hosts adapt their binding site to different guests in order to optimize the fraction of occupied space. Once a binding geometry is established, it is characterized by a very low degree of flexibility. The guest-hosting properties of both molecules can be suspended by an external stimulus: addition of acid induces an opening of portals in the structures and immediately releases all bound cargo. Neutralization of the solution completely restores the initial state.

1. Introduction

Molecular-scale functional systems[1] have emerged in eclectic variety since Feynman's fundamental reflections on such machinery.[2] They are targeted at an enormous number of innovative applications in fields such as materials and catalysis, energy harvesting, information storage and processing, or targeted delivery and transport. Molecular switches are one such type of device:[3] external stimuli can be used to toggle between distinct stable states with different properties.

A particularly effective strategy in the construction of molecular switches for exerting dynamic control over physical properties is to provoke changes in molecular geometry:[4] to just name examples, motion in interlocked molecules can modify their fluorescence or conductivity and allow for the construction of macroscopic Boolean logic gates[4r] or nanoelectromechanical memory devices,[4l,v] whereas light can be used to induce unidirectional rotation in three-state chiroptical switches,[4h,k] which then directs the twist sense of helical polymers.[4u] Provoking a geometry change in rotaxanes or diarylethene molecular switches[4j] can control, among other materials properties, the water repellency of surfaces.[4s,t]

Controlled mechanical motion has also been exploited to modulate the guest-hosting properties of molecular (nano)systems, whereby allosteric[4a] and photoresponsive[4b,c] crown ethers represent classical examples. Most recently, (pseudo)rotaxane molecules attached to the surface of mesoporous silica have been reported. The molecular switches act as gatekeepers and allow encapsulation of guest molecules within the pores of nanoparticles; stimulation results in controlled release.[5]

Among switchable receptors are also the resorcin[4]arene cavitands, introduced by Cram et al. in 1982 (Scheme 1).[6] At room temperature and in organic solvents, the cavitands are exclusively present in the *vase* conformation, whereas lowering the temperature[7] or adding metal ions[8] or acid[9] converts the molecules to the open, flat *kite* form. This controllable transformation has recently been applied in the construction of molecular switches that undergo precisely defined multi-nanometer expansion/contraction movements.[10]

In their pristine quinoxaline-bridged guise, the cavitands are in principle capable of accepting guest molecules within their concave

* Corresponding author. Tel.: +41 44 632 2992; fax: +41 44 632 1109.
E-mail address: diederich@org.chem.ethz.ch (F. Diederich).

0040-4020/$ – see front matter © 2008 Elsevier Ltd. All rights reserved.
doi:10.1016/j.tet.2008.04.102

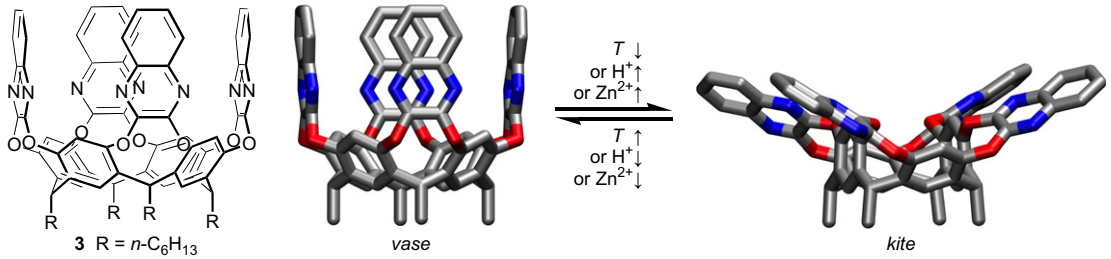

Scheme 1. Structural representation for the tetraquinoxaline-bridged cavitand **3** and molecular models (MOPAC2007, PM6), illustrating the *vase–kite* equilibrium. The cavitand can be switched to the *kite* conformation by lowering the temperature or by the addition of acid or metal ions.

interior.[11] Still, as a consequence of their open-top geometry and conformational flexibility, binding is weak and guest exchange proceeds rapidly in the absence of additional rim functionalization.[12] Closed-shell structures enforcing an interior cavity do on the other hand allow for the formation of stable and inert encapsulation complexes. Uptake and release of smaller molecules into and from these containers are then, however, difficult to control dynamically because exchange kinetics are a function of host structure: covalently closed surfaces completely inhibit guest exchange, while the introduction of shell holes of appropriate size can allow for entrance and egress of smaller species.[13] Self-assembled capsules[14] and cages[15] do additionally impose their own association–dissociation dynamics on the exchange kinetics of their encapsulation complexes,[13j,k,16] and approaches to exert dynamic control over guest uptake and release properties of enforced inner phases have targeted influencing the self-assembly of supramolecular structures.[14b,j]

Herein, we report on the syntheses and on extensive binding, molecular dynamics, and switching studies of the switchable baskets **1** and **2** (Scheme 2), resorcin[4]arene-based container molecules that accommodate suitable guests within well-defined cavities and completely surround them. The molecules show remarkable binding selectivity as a consequence of their precisely defined geometry. Portals delimiting the cavity are opened upon the addition of acid and binding is suspended as a result of the induced change in structure. The process is fully reversible; neutralization of the solution completely recovers the initial state.[17]

2. Results and discussion

2.1. Container molecules with portals based on a resorcin[4]arene platform

The switchable baskets **1** and **2** are constructed from a resorcin[4]arene bowl, to which two quinoxaline flaps are appended in *anti*-orientation (Scheme 2 and Fig. 1). Two diazaphthalimide walls are connected to each other by a rigid hexa-2,4-diyne-1,6-diyl bridge in the case of **1** and by an octa-3,5-diyne-1,8-diyl unit in **2**. The acetylenic connections cap-off the baskets and enforce precisely defined cavities within **1** and **2**.

Pairs of adjacent phenol ethers, by which the quinoxaline flaps are attached to the resorcin[4]arene bowl, act as hinges to open these portals in the switching process. However, the barrier for the required flip of the constrained nine-membered ring (Scheme 2, highlighted in red) is high[9b] and at room temperature in solvents such as acetone-d_6, $CDCl_3$, or mesitylene-d_{12}, the molecules are exclusively present in their *closed* conformations.[7,9b]

To assess the degree of rigidification caused by bridging the cavitand structure with alkyne bridges, we have performed molecular dynamics experiments (1000 ps simulation time with 1.0 fs time steps, MMFF94s force field, 300 K, GB/SA model for $CHCl_3$, MacroModel 9.5).[18] Figure 2 compares the local conformational space of *vase*-**3**, lacking any rim bridging, and the *closed* conformer of **1**. It is clear that the *vase* form of the tetraquinoxaline-bridged cavitand **3** is poorly defined because the walls are subjected to enormous fluctuation. In sharp contrast, *closed*-**1** exhibits a highly restricted local conformational space. The acetylenic bridge enforces the structure as a whole, including bowl and portals; a precisely defined cavity results.

2.2. Synthesis and purification

The key step in the synthesis of **1** and **2** is an oxidative acetylenic coupling reaction of open-top precursor cavitands **4** and **5** (Scheme 2). Intramolecular coupling of **5** affords the basket **2** along with a dimeric structure, the switchable tube **6**, in a ratio of **2**/**6** ≈ 10:1. The two products can be separated by preparative high-performance gel-permeation chromatography (GPC).[17] Precursor **4** does not give isolable quantities of a dimerization product under the coupling conditions, most probably because the resulting tube would be too strained. The open-top precursor molecules are formed by bridging the bis-*anti*-quinoxaline cavitand **7**[19] with the propynyl- or butynyl-substituted 2,3-dichlorodiazapthalimide **8** and **9**, respectively (Scheme 3). Synthesis of these wall units proceeds, in the case of **8**, via condensation of 2,3-dichloropyrazine-5,6-dicarboxylic acid anhydride[20] with propargylic amine **10**, or for

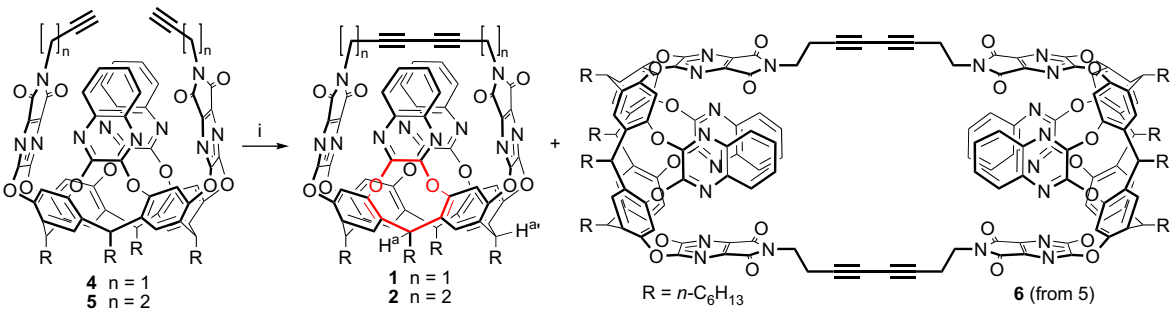

Scheme 2. Synthesis of switchable container molecules. (i) CuCl, $CuCl_2$, DMF, 17 h; 20% (**1**), 31% (**2**), 6% (**6**).

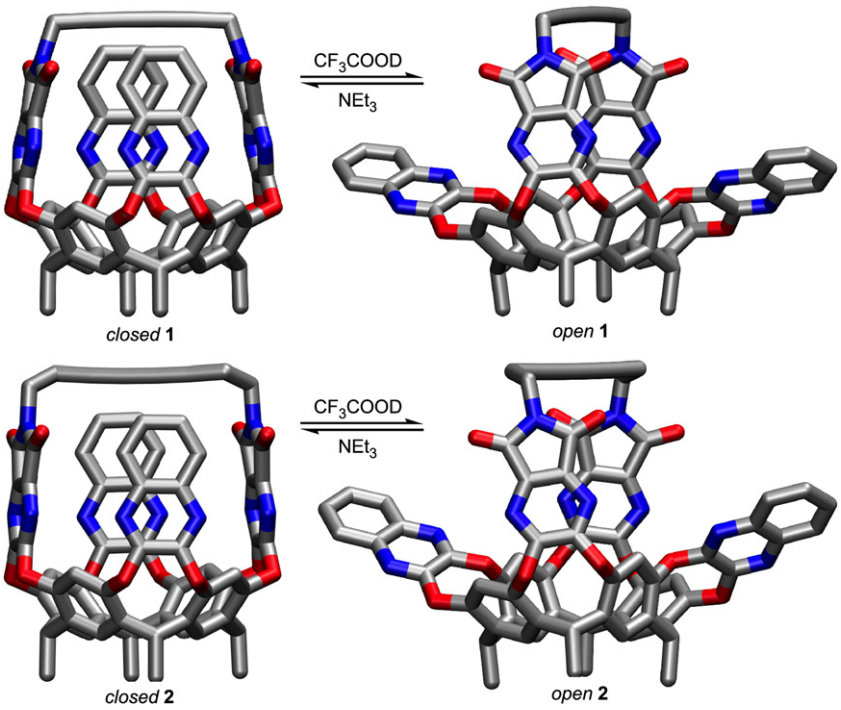

Figure 1. Molecular models (MOPAC2007, PM6) for the *closed* and *open* conformations of **1** and **2**. The equilibria can be controlled by adjusting [H^+] in their solutions. Legs and hydrogen atoms are omitted.

9, by Mitsunobu-reaction[21] of 2,3-dichlorodiazapthalimide[22] with homopropargylic alcohol **11**.

GPC separation of basket **2** and tube **6** in $CHCl_3$ (HPLC grade) gave both compounds in high chemical purity as determined by analytical GPC as well as ^1H and ^{13}C NMR spectroscopies in $CDCl_3$. In acetone-d_6, it became apparent that the sample of container **2** contained traces of residual $CHCl_3$ after drying (10^{-2} mbar, >24 h, 298 K). We usually perform host–guest complexation studies on these systems in mesitylene-d_{12}, which is the largest commercially available deuterated solvent. It is too large to enter the cavity of the baskets and does not compete for binding.[7b,9b,14c] Recording an ^1H NMR spectrum of **2** in this solvent showed only one set of host signals (Fig. 3a). We therefore concluded initially that residual $CHCl_3$ is either not encapsulated or only weakly, with host–guest exchange being rapid on the NMR chemical shift time scale.

In the case of **1**, purification by GPC is not necessary and, after work-up, we subjected the crude product to flash chromatography in distilled technical grade CH_2Cl_2. Again, analytical GPC as well as ^1H and ^{13}C NMR spectroscopies in $CDCl_3$ indicated the presence of only one host species. In mesitylene-d_{12}, however, several sets of host signals were observed. We initially attributed these to bound impurities from the technical solvent. Using high-purity CH_2Cl_2 ('Baker analyzed' grade) for separation and drying the sample for 10 days at 10^{-2} mbar (298 K) still left us with two sets of host signals in ^1H NMR spectra, recorded in carefully distilled mesitylene-d_{12} (Fig. 3d). It turned out that one set of signals corresponded to free **1**, whereas the second set was caused by the inclusion complex $CH_2Cl_2\subset$**1**. To attain a clear view on only the host resonances, we bubbled Ar for 58 h at 298 K through a solution of **1** in distilled mesitylene-d_{12}, which purged the CH_2Cl_2 impurity (Fig. 3e).[23]

In preparation of comparative host–guest chemistry studies, we had to ensure consistency between the baskets **1** and **2** in terms of sample preparation and solvent used for purification. We therefore subjected the crude product mixture of **2** and **6** to medium pressure liquid chromatography (MPLC) in CH_2Cl_2 ('Baker analyzed' grade). Although this treatment is not effective for obtaining pure tube **6**, we were able to separate a homogenous sample of **2**. In contrast to what we had observed previously, the ^1H NMR spectrum of this sample in distilled mesitylene-d_{12} showed only broad featureless

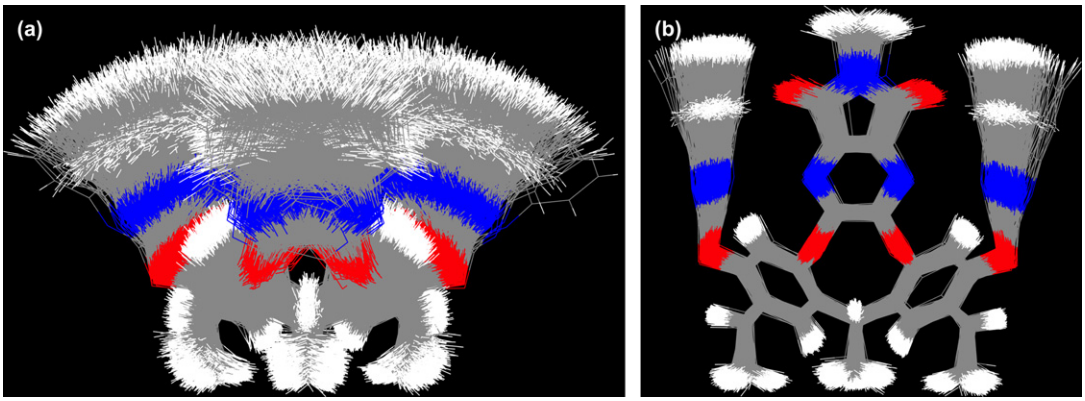

Figure 2. Overlays of 1000 structures of *vase*-**3** (a) and *closed*-**1** (b), sampled from molecular dynamics simulations. In both cases, the hexyl legs were substituted for methyl groups. Whereas the structure of *vase*-**3** is subjected to pronounced fluctuation, the local conformational space of *closed*-**1** is very restricted.

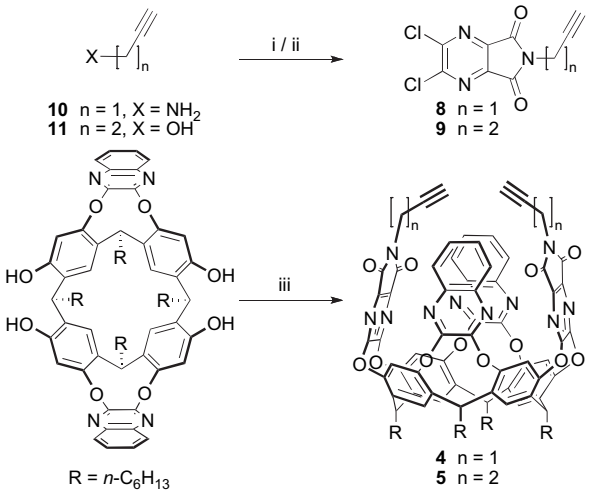

Scheme 3. Synthesis of the precursor cavitands **4** and **5**. (i) 5,6-Dichloropyrazine-2,3-dicarboxylic acid anhydride, $(COCl)_2$, THF, 17 h; 40% (**8**). (ii) PPh_3, diethyl azodicarboxylate, 5,6-dichloropyrazine-2,3-dicarboxylic acid anhydride, THF, 20 h; 48% (**9**). (iii) **8** or **9**, *i*-Pr_2NEt, DMF, 17 h, 40 °C; 60% (**4**), 62% (**5**).

signals (Fig. 3b). We attribute this behavior to the larger conformational space of **2** as compared to **1**. The additional two methylene groups in the bridge allow for different conformations, which in our interpretation interconvert and have lifetimes comparable to the NMR time scale (500 MHz, 298 K). Gradually heating the sample to 350 K allowed the observation of one set of well-resolved resonances (these spectra are reproduced in Supplementary data). Addition of $CHCl_3$ to the sample at 298 K did also resolve the spectrum: the basket binds the guest and its structure is stabilized (Fig. 3c). These sharp resonances were identical to what we had considered free host in all our earlier experiments (Fig. 3a), which only allows the conclusion that we had previously dealt[17] with host **2**, fully occupied by residual $CHCl_3$.

Identically treated samples of **1** and **2** were then used to quantify the amount and nature of impurities present, as well as to estimate the association constants of their encapsulation complexes. Both containers were purified in CH_2Cl_2 ('Baker analyzed' grade) and dried for 10 days at 10^{-2} mbar (298 K). We then added cycloalkane guests in excess to their solutions in carefully distilled mesitylene-d_{12}, cyclohexane in the case of **2** and cyclopentane in the case of **1**. These are bound more strongly than the halogenated solvents and therefore expel them from the cavity. In both cases, one well-resolved set of signals resulted and all resonances corresponded to the baskets fully occupied by cycloalkane guest. In addition, one sharp singlet at δ=4.3 ppm (^{1}H NMR, distilled mesitylene-d_{12}) was present, caused by free CH_2Cl_2 (Fig. 3f).[24] Integration of this signal revealed stoichiometries of **1**·0.55 CH_2Cl_2 and **2**·0.50 CH_2Cl_2—an assignment, which was corroborated by elemental analysis. Further decrease in the amount of residual solvent is extremely slow (see Supplementary data): prolonging the drying time to 25 days still leaves behind 0.48 equiv CH_2Cl_2 in the case of **1**. All experiments described here were carried out after 10 days of drying, i.e., on samples containing 0.50 equiv CH_2Cl_2 for **2** and 0.55 equiv for **1**. This amount of residual solvent corresponds to about 200 nL in a typical NMR experiment. Knowing the concentrations of all species present in the different solutions, we were able to deduce association constants for halogenated solvents in distilled mesitylene-d_{12}: K_a ($CH_2Cl_2\subset$**1**)=0.2×10^3 M^{-1}, K_a ($CH_2Cl_2\subset$**2**)=0.5×10^3 M^{-1}, and K_a ($CHCl_3\subset$**2**)=1×10^3 M^{-1}.

2.3. Host–guest chemistry

In the earlier communication, we had established that **2** binds cycloalkane guests under enthalpy control.[17] The container completely surrounds its encapsulated cargo and causes large diamagnetic shifts for the hydrogen atom resonances of included molecules (^{1}H NMR signals for encapsulated cycloalkanes appear at around −3 ppm, see Fig. 3f). According to current knowledge, guest exchange requires the opening of at least one portal[25] and therefore a conformational flip of the constrained nine-membered ring, which connects the bowl to a quinoxaline flap (Scheme 2, highlighted in red). In accordance with this, we observed a sizeable enthalpic barrier to guest self-exchange. We have also reported that **2** is highly selective and prefers to encapsulate cyclohexane over its homologous cycloalkanes. This behavior is still clearly observed, as a comparison of the apparent association constants (K_{app}) for the guests with **2** in distilled mesitylene-d_{12} (Table 1) indicates: cyclohexane is bound most strongly in this series and with K_{app}=(41±9.9)×10^3 M^{-1} it is preferred by **2** over cyclopentane, for which K_{app}=(24±7.1)×10^3 M^{-1} results. Cycloheptane is bound much more weakly, as the value of K_{app}=(0.96±0.30)×10^3 M^{-1} shows. The absolute values are about 10-fold higher compared to those measured earlier[17] on the $CHCl_3$-occupied samples and certainly on the upper limit of what can be determined from integration of ^{1}H NMR spectra at slow exchange. As discussed, all apparent association constants given in this account are measured in the presence of ≈0.5 equiv residual CH_2Cl_2 and possibly other binding impurities below the detection threshold of ^{1}H NMR spectroscopy. However, the values are comparable to each other because the amount of impurities present is the same in all experiments reported here.

Container **1** is slightly smaller than **2**. Determining the apparent association constants for cycloalkanes with **1** (Table 1) allowed us

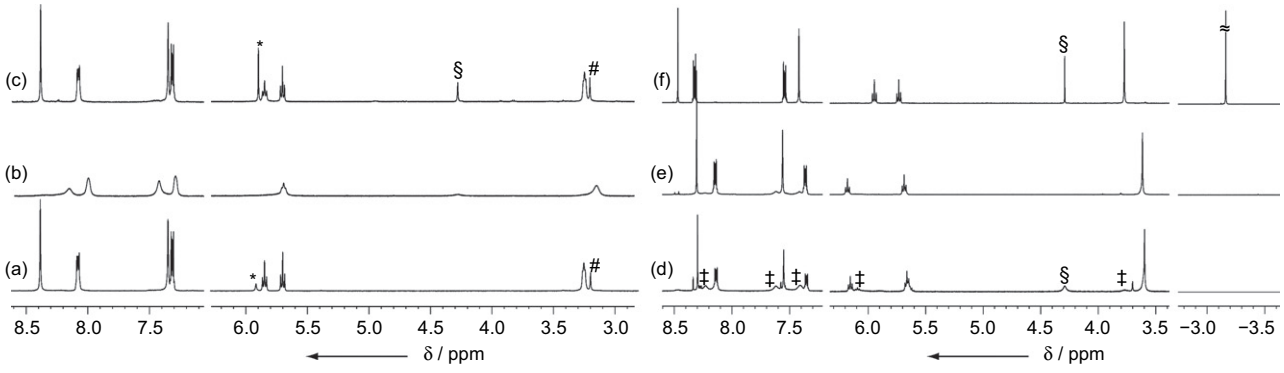

Figure 3. Portions of ^{1}H NMR spectra (500 MHz, 298 K, mesitylene-d_{12}). Basket **2** after separation by preparative GPC in $CHCl_3$ (a), after separation by flash chromatography in CH_2Cl_2 (b), and after separation by flash chromatography in CH_2Cl_2 and addition of 2 equiv $CHCl_3$ (c). Basket **1** after separation by flash chromatography in CH_2Cl_2 (d), after separation by flash chromatography in CH_2Cl_2 and purging with Ar for 58 h at 298 K (e), and after separation by flash chromatography in CH_2Cl_2 and addition of 3 equiv cyclopentane (f). The encapsulated guest appears at −3.16 ppm; *: free $CHCl_3$; #: bound $CHCl_3$; §: free CH_2Cl_2; ‡: $CH_2Cl_2\subset$**1**.

Table 1
Packing coefficients, apparent association constants, and thermodynamic parameters determined by van't Hoff analysis of VT-NMR data for encapsulation compounds

Complex	PC_{static}	PC_{MD}	K_{app} (10^3 M^{-1})[a]	ΔG^{298K} (kcal mol^{-1})[b]	ΔH (kcal mol^{-1})	ΔS (cal K^{-1})
Cyclobutane⊂**1**	0.48	0.47±0.04	0.95±0.12	−4.1±0.08	—[c]	—[c]
Cyclopentane⊂**1**	0.58	0.53±0.04	9.7±0.84	−5.4±0.05	−6.3±0.28	−3.1±0.85
Cyclohexane⊂**1**	0.70	0.61±0.05	2.3±0.32	−4.6±0.09	−5.3±0.20	−2.3±0.48
Oxacyclobutane⊂**1**	0.42	—[d]	weak[e]	—[e]	—[e]	—[e]
Oxacyclopentane⊂**1**	0.53	—[d]	24±4.5	−6.0±0.12	−8.0±0.70	−6.8±1.38
Oxacyclohexane⊂**1**	0.64	—[d]	48±5.8	−6.4±0.08	−8.7±0.55	−7.5±1.70
Oxacycloheptane⊂**1**	0.76	—[d]	3.7±0.85	−4.9±0.15	−7.1±0.35	−7.5±1.08
Cyclobutane⊂**2**	0.38	0.44±0.04	1.1±0.26	−4.1±0.16	—[c]	—[c]
Cyclopentane⊂**2**	0.46	0.52±0.04	24±7.1	−6.0±0.21	−10±0.59	−15±1.8
Cyclohexane⊂**2**	0.55	0.54±0.05	41±9.9	−6.3±0.16	−12±0.52	−19±1.6
Cycloheptane⊂**2**	0.64	0.61±0.05	0.96±0.30	−4.1±0.22	−7.9±0.21	−13±0.64

All measurements were conducted in distilled mesitylene-d_{12}.
[a] Determined by integration of ^{1}H NMR spectra at slow exchange.
[b] Calculated from K_{app}.
[c] Although solutions of cyclobutane (bp 12 °C) in mesitylene-d_{12} were found stable enough to determine K_{app}, the concentration was not stable in variable temperature (VT) experiments: all VT experiments were conducted in the order of increasing temperatures, and, after cooling down to room temperature again, the concentration of the guests was checked. For all guests except cyclobutane, no significant evaporation was observed.
[d] Not determined.
[e] Binding is too weak to accurately determine K_{app}.

to observe a shift in selectivity: with $K_{app}=(9.7\pm0.84)\times10^3$ M^{-1}, cyclopentane is in this case preferred over cyclobutane ($K_{app}=(0.95\pm0.12)\times10^3$ M^{-1}) and cyclohexane with $K_{app}=(2.3\pm0.32)\times10^3$ M^{-1}. Cycloheptane is not bound. To rationalize this selectivity, we have calculated the packing coefficients (PCs) for the encapsulation complexes and applied the so-called 55% rule. This solution, elegantly elaborated by Mecozzi and Rebek, applies to apolar binding events and says that a molecule-within-molecule complex is favored, when the guest fills 55±9% of the available space (PC=0.55±0.09).[26] Tighter ensembles have to invest too much of their translational and rotational freedoms in the binding event, whereas in looser complexes, the guest fails to maximize the enthalpic benefits of nestling to the inner host surface. The rule has been validated in a number of synthetic host–guest systems,[12b,27] and we have recently applied it to an enzyme environment.[28]

To determine the packing coefficients, the molecular volume of the guest and the volume of the available cavity have to be calculated. We previously performed these calculations by the so-called cavity-filling method.[26,28] This means that a tight hydrocarbon network is constructed inside the host. If a molecular modeling package is used, which does not count overlapping volumes twice, subtracting the volume of the empty host from the volume of the container with the network inside delivers a good estimate for the space within. A slightly different approach to determine interior volumes is implemented in software packages used in structural biology, such as Voidoo:[29] the cavity is filled with spherical probes that are positioned on a grid and all non-overlapping volumes that can be occupied are summed up. Employing the latter method and the atomic radii of Bondi,[30] which are particularly suitable for volume considerations, the cavity size of **1** was determined as 145 Å^3, whereas **2** has 184 Å^3 of space on the inside. The cavities determined by these methods are illustrated in Figure 4.

It has to be pointed out here that using different sets of atomic radii will deliver different cavity volumes, different guest volumes, and possibly different packing coefficients. However, the absolute value of 0.55 as an optimum packing coefficient is less central than the fact that there is an optimum packing coefficient for series of inclusion complexes. Relating quantitative binding data to PCs determined by the same method using the same parameters and atomic radii is, however, a very suitable approach to gain important and fundamental insights into the molecular recognition properties of pockets and cavities.

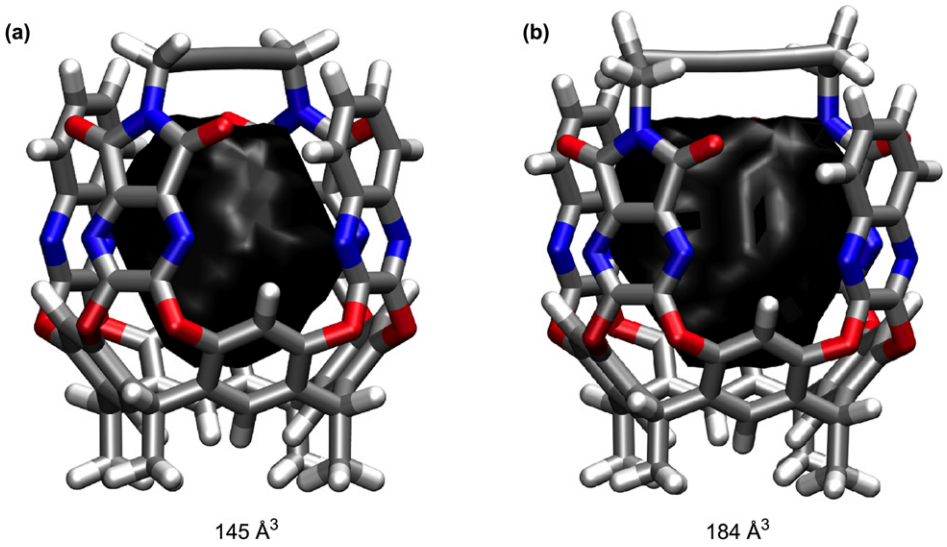

Figure 4. Visualization of the available cavity space within models for **1** (a) and **2** (b). The geometries were optimized with MOPAC2007 (PM6) and the cavity volumes were determined with Voidoo. Hexyl legs were substituted for methyl groups.

In this case, determining the packing coefficients of our complexes with both methods outlined above gave essentially the same results: cyclohexane occupies 55% of the space within **2** when volumes are calculated with Voidoo, whereas the cavity-filling method gives 56%. Cyclopentane fills 46% (47%), whereas cycloheptane needs 64% (65%). Cyclooctane, corresponding to 72% cavity occupation, is not bound.

Host **1** differs only by a subtle structural modification: on each side of the butadiyne unit, the bridge comprises one methylene group less. This difference has consequences on the cavity volume and therefore on binding selectivity. Cyclopentane, filling 58% (given are results from Voidoo, the values obtained by the cavity-filling method are similar) of the interior, is now the preferred binder. Cyclobutane (48%) and cyclohexane (70%) are bound significantly weaker. An encapsulation complex of **1** with cycloheptane would correspond to 81% occupation and is not formed.

The quality of attractive interactions between host and guest is clearly dependent on cavity occupation. This is evident from the relative apparent association constants as discussed above, but also from different behavior of cyclohexane inside the two baskets at lowered temperature. We cooled a solution of cyclohexane in acetone-d_6 to 189 K, where the axial and equatorial hydrogen atoms give different signals in 300 MHz ^{1}H NMR spectra. From the separation of the resonances ($\Delta\nu$) and the temperature, at which the signals coalesce upon warming up (T_c), the activation barrier for chair inversion at coalescence ($\Delta G_c^{\neq}$) can be calculated.[31] For cyclohexane in acetone, we determined this value as $\Delta G_c^{\neq}=10.31\pm0.05$ kcal mol^{-1} ($\Delta\nu=142$ Hz, $T_c=228$ K), which compares well with the literature data.[31b] For cyclohexane encapsulated within **1**, we observed no significant change in $\Delta G_c^{\neq}$, which now amounts to 10.34 ± 0.05 kcal mol^{-1} ($\Delta\nu=301$ Hz, $T_c=236$ K). Cyclohexane bound in the cavity of **2**, however, shows a small but significant increase for the barrier to ring inversion $\Delta G_c^{\neq}=10.56\pm0.05$ kcal mol^{-1} ($\Delta\nu=209$ Hz, $T_c=237$ K). The observed additional activation free enthalpy of $\Delta\Delta G_c^{\neq}=0.25\pm0.10$ kcal mol^{-1} that is required for the ring flip inside only the larger container is similar to what Rebek et al. have observed for cyclohexane inside a dimeric host (the so-called 'Jelly Doughnut'). The increase in activation energy for cyclohexane ring inversion was attributed by them to favorable interaction of the host with the ground state of cyclohexane.[32]

Only the larger **2**, in which cyclohexane does optimally fill the cavity, stabilizes the chair conformation to the extent that an increase in $\Delta G_c^{\neq}$ is observed. Cyclohexane$\subset$**1** is packed too tightly; stabilization of the chair is less pronounced and does not effect a change in $\Delta G_c^{\neq}$. The larger frequency separation $\Delta\nu$ inside **1** is indicative of an anisotropic effect: interaction of the host with axial and equatorial hydrogen atoms of cyclohexane is more different in the case of **1**, which is presumably caused by a preferred position of the guest inside the cavity. Rotation of the guest around its C_2 axes must be more restrained in the smaller **1** as a consequence of the higher packing coefficient.

The electronic environment within the cavity of both container molecules is not isotropic. The bottom, with the resorcin[4]arene bowl, is quite electron rich. In contrast, the upper part has a more electron-deficient surrounding, with the two quinoxaline portals, the butadiyne bridge, and in particular the two rigid diazaphthalimide walls. Hence, we added a series of cyclic ethers to container **1** in distilled mesitylene-d_{12} to evaluate if interaction of their electron-rich oxygen atoms with the upper part of the cavity leads to a preferred orientation of the bound guests and provides for additional stabilization of the encapsulation complexes. In this series, oxacyclohexane (tetrahydropyran) is bound with a 20-fold higher apparent association constant than its carbocyclic analogue and gives the strongest complex of the series with $K_{app}=(48\pm5.8)\times10^3$ M^{-1} (Table 1). The cavity occupation is 64%. Oxacyclopentane (tetrahydrofuran, 53% occupation, $K_{app}=(24\pm4.5)\times10^3$ M^{-1}) is bound more weakly than its larger homologue, but still twice as well as cyclopentane. Oxacyclobutane (oxetane, 42%) is only weakly bound, while significant encapsulation of oxacycloheptane (oxepane, 76%) is still observed with $K_{app}=(3.7\pm0.85)\times10^3$ M^{-1}. When additional polar stabilization, such as dipolar $C_2O\cdots C{=}O$ interactions between guest and the imide moieties,[33] complements the C–H$\cdots\pi$ interactions in such molecule-within-molecule complexes, association is clearly enhanced. The optimum cavity occupation seems higher; slightly tighter complexes seem to be preferred. However, K_{app} values for the cyclic ethers in **1** are on the upper limit of what can be determined by integration of NMR spectra at slow exchange and the resulting errors are sizeable. Binding of the ethers in **2** is so strong that meaningful data could not be derived from integration of ^{1}H NMR spectra. Further quantitative work to clarify the influence of different associative interactions on the optimum packing coefficient in encapsulation complexes is therefore clearly necessary.

A distinct geometrical preference for oxacyclohexane binding in **1** was unambiguously detected by an ^{1}H–^{1}H rotating-frame Overhauser spectroscopy (ROESY) experiment (500 MHz, 300 K, mesitylene-d_{12}; a reproduction of the spectrum is contained in Supplementary data): cross-peaks appeared between the signals for hydrogen atoms in 4-position of oxacyclohexane (H^4) and the resonances for aromatic hydrogen atoms in the resorcinarene bowl, but not between signals for H^4 and the methylene hydrogens in the hexadiyne bridge (H^f). Cross-peaks between signals for oxacyclohexane $H^{2/6}$ and the methine protons of the container ($H^{a/a'}$) were not visible, instead a strong correlation between $H^{2/6}$ and H^f was observed. These results reveal an orientation of the guest, which interacts with its ether oxygen atom more favorably with the more electron-deficient upper cavity environment. In addition, the appearance of cross-peaks between signals for H^4 and the methine protons underneath the imide walls ($H^{a'}$) but not to those underneath the quinoxaline portals (H^a) indicates a preferred orientation of the guest parallel to the diazaphthalimide moieties, presumably caused by attractive dipolar $C_2O\cdots C{=}O$ interactions between guest and host.[33]

To further characterize the binding events, we determined the thermodynamic parameters for three series of encapsulation compounds: cycloalkanes within **1** and **2**, as well as the cyclic ethers within **1**. The results obtained by van't Hoff analysis of variable temperature ^{1}H NMR data in distilled mesitylene-d_{12} are summarized in Table 1. Binding is clearly enthalpy-driven, with ΔH values between -5 and -12 kcal mol^{-1}. The entropic costs for encapsulation were measured as -2 to -20 cal mol^{-1} K^{-1}, corresponding to values for $T\Delta S$ at 298 K between -1 and -7 kcal mol^{-1}. We were interested in whether tighter ensembles pay relatively higher entropic costs, as compared to the most favorable combinations, so we plotted ΔH against ΔS for complexes of both **1** and **2** (Fig. 5). Linear regression over all data points is indicative of a situation subjected to enthalpy–entropy compensation.[34] Thermodynamic data do not indicate sizeable correlation between cavity occupation and relatively higher or lower entropic penalties in the formation of molecule-within-molecule complexes.

For the determination of the packing coefficients, we had used molecular structures for the containers that were optimized with the semiempirical PM6 method as implemented in MOPAC2007.[35] Certainly, the determination of void volumes in static structures is intrinsically approximative with respect to packing in encapsulation complexes because, as shown in Figure 2b, the molecules are subjected to some degree of conformational fluctuation and guest binding can also affect geometrical changes.

Molecular Dynamics (MD) simulations allow the evaluation of molecular geometry under consideration of thermal fluctuation, and we have employed such methods to assess the rigidification that results from the acetylenic bridge in **1** (see above). Using MD

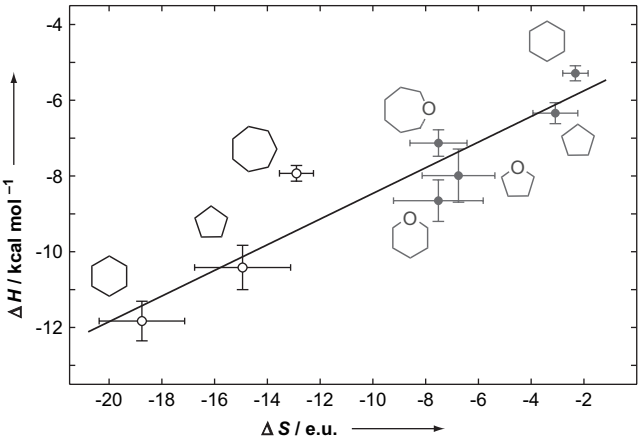

Figure 5. Enthalpy–entropy compensation. Thermodynamic parameters are plotted for encapsulation complexes with **1** (filled circles) and **2** (empty circles).

simulations, we wanted to further complement the determination of packing coefficients and overcome the approximative nature of void volume calculations on static structures. We were also interested to what extent guest binding within our baskets is mediated by an induced-fit behavior.

Therefore, we subjected both series of cycloalkane encapsulation compounds to MD experiments (1000 ps simulations with 1.0 fs time steps, MMFF94s force field, 300 K, GB/SA model for $CHCl_3$, MacroModel 9.5).[18] For each of the complexes, we sampled 1000 structures over the simulation time, removed the guest molecules, and submitted all resulting host geometries to the program Voidoo.[29] The time-averaged cavity sizes further corroborate that geometry and binding site of the baskets are not subjected to pronounced fluctuation, but depending on the guest size, the binding event is characterized by some degree of induced-fit behavior.

For the preferred complexes cyclopentane⊂**1** and cyclohexane⊂**2**, packing coefficients of PC_{static}=0.58 and PC_{static}=0.55 were determined on the static structures. Results from the dynamics runs give values of PC_{MD}=0.53±0.04 and PC_{MD}=0.52±0.04, respectively. The best binders fill identical fractions of the interior space. Once the host has accepted a guest, the cavity size is locked, as indicated by the small standard deviations over all processed structures. Cyclobutane⊂**1** shows no adaptation of the container to the guest (PC_{static}=0.48, PC_{MD}=0.47±0.03), whereas in the tighter complex cyclohexane⊂**1** (PC_{static}=0.70) some widening of the cavity is enforced (PC_{MD}=0.61±0.05). A cavity occupation of 70% is not tolerated and the molecule has to expand its structure in order to accept the guest. For the larger container, a very similar picture emerges: formation of cyclobutane⊂**2** (PC_{static}=0.38, PC_{MD}=0.44±0.04) induces some contraction of the host, although only to a limited extent. Cyclopentane⊂**2** (PC_{static}=0.46, PC_{MD}=0.52 ± 0.04) also causes the larger container to slightly reduce its cavity size, whereas in cycloheptane⊂**2** (PC_{static}=0.64, PC_{MD}=0.61±0.05) we observe minimal time-averaged widening.

Thus, molecular dynamics experiments reveal that the containers can adjust their geometry, if this leads to more favorable filling of space. Other cases are known where the guests also adapt in order to fill an optimum fraction of a cavity.[12b,27a,f,28,36] Linear alkane chains, e.g., which are too long to be encapsulated in a given space, will assume unfavorable *gauche* conformations, if the resulting encapsulation complexes have favorable packing coefficients.

In the cases studied here, the guests cannot change their volume significantly. The hosts adjust to the different guests, but the adaptability is limited, with PCs changing by less than 0.1. Changes in cavity size require the quinoxaline flaps to move inward or outward; in both cases, the host molecules have to move away from their lowest-energy geometries and strain is introduced. For the best binders in the two series of encapsulation compounds studied here, packing coefficients closest to 0.55 were determined on the static structures and K_{app} of $10^4\ M^{-1}$ are only observed when the adapted complex lies in the narrow range of 52–54% cavity occupation. For host–guest combinations that lie somewhat away from the optimum filling of space, the hosts contract or expand, in order to come closest to an optimum value for cavity occupation—until the costs for further adjustment would jeopardize the enthalpic gain of the binding event. As a consequence, packing coefficients determined on the static thermodynamic minimum structures represent a good estimate for the time-averaged situation, at least for the relatively rigid systems studied here.

2.4. Conformational switching and reversibly controllable guest encapsulation

A key property of resorcin[4]arene cavitands is their ability to reversibly change their conformation upon stimulation. When a solution of the tetraquinoxaline-bridged cavitand **3** is treated with CF_3COOH, the equilibrium between *vase*-**3** and *kite*-**3** is completely shifted to the open conformation. Protonation of the mildly basic quinoxaline nitrogen atoms introduces positive charges that repel each other.[9] As a consequence, the nine-membered rings connecting the quinoxaline walls to the bowl flip over and the flaps assume the sprawled out positions illustrated in Scheme 1.[37] This conformational change is commonly monitored by the highly diagnostic ^1H NMR signal for the methine protons underneath the quinoxaline walls (H^a, see Scheme 2).[7a,9] The resonance appears at rather low field in *vase*-**3** (δ=5.56 ppm, $CDCl_3$, 298 K) because the protons are located in the deshielding zone of the neighboring aromatic rings. When the solution is acidified with increasing amounts of CF_3COOH up to a concentration of 0.4 M, the methine resonance moves gradually upfield and comes to stand at δ=3.80 ppm, which is indicative of fully opened structures, as comparison with *kite*-locked resorcin[4]arenes such as velcrands[20,38] (δ=3.52 ppm) or an octanitro derivative[19a] (δ=3.90–3.96 ppm) shows.

A major objective in the design of **1** and **2** was to preserve two quinoxaline walls as gates to open the cavities. To characterize the behavior of our containers in this respect, we titrated solutions of **1** and **2** in different solvents with CF_3COOD and monitored the position of the ^1H NMR signals (500 MHz, 298 K) for H^a (underneath the quinoxaline walls, red lines in Fig. 6) and for $H^{a'}$ (underneath the rigid imide walls, blue lines). It turned out that in both $CDCl_3$ (dashed lines) and CD_2Cl_2 (solid lines), for both **1** (triangles) and **2** (circles), the resonance for $H^{a'}$ did only marginally change position

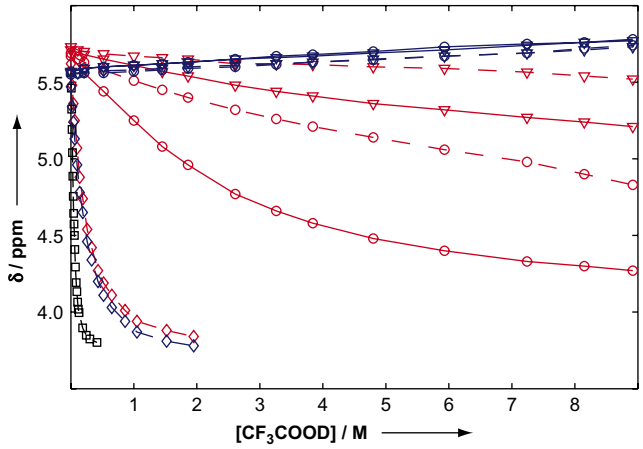

Figure 6. Switching profiles of the container molecules **1** (triangles) and **2** (circles), as well as, for comparison, for precursors **4** (diamonds) and **3** (squares) in $CDCl_3$ (dashed lines) and CD_2Cl_2 (solid lines). Blue: resonance of $H^{a'}$ underneath the imide walls; red: resonance of H^a underneath the quinoxaline gates.

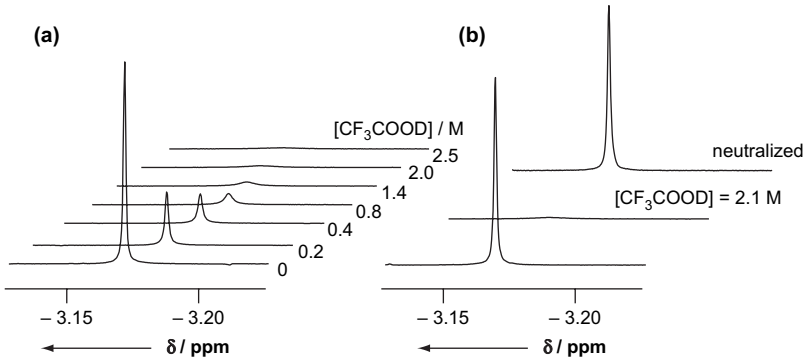

Figure 7. Reversibly controllable guest encapsulation within **1**. Shown is the ^{1}H NMR signal (500 MHz, 300 K, mesitylene-d_{12}) for bound cyclopentane ([**1**]≈3.5 mM, 0.5 equiv guest present). (a) Increasing amounts of CF_3COOD are added and the guest is released. (b) After acid addition, neutralization of the solution with NEt_3 immediately and completely restores binding. An ionic liquid is formed by the salt, which was removed by syringe prior to data acquisition.

upon acidification, indicating that the bridged walls above these hydrogen atoms are indeed rigid and cannot move outward.

For H^a, a different picture emerged: in CD_2Cl_2, this resonance for the larger **2** did slowly move upfield, with a maximum chemical shift difference of $\Delta\delta=-1.40$ ppm. The magnitude of this value is comparable to the open-top cavitands ($\Delta\delta=-1.78$ ppm in the case of **4**) and indicates almost complete opening of the flaps with essentially exclusive population of the *open* conformations. Instead of [CF_3COOD]=0.4 M, however, a concentration of 9 M is required. Owing to the rigidified framework, opening induces substantial strain in **2** and the process is more difficult to effect as compared to the unbridged structures. Basket **1** is more rigid and, in accordance, it is even more difficult to shift the equilibrium from *closed* to *open*: in CD_2Cl_2, signals for H^a moved by $\Delta\delta=-0.50$ ppm at [CF_3COOD]=9 M.

In addition, solvent effects have to be considered: CD_2Cl_2 is bound by both containers, which works in favor of the *closed* forms.[9b] Such stabilization can be observed to a higher extent when the baskets are switched in $CDCl_3$, which fits very well in the cavities (the solvent occupies 38% of the space within **2** and 49% in the case of **1**). In this case, the resonance for H^a in **2** changes position by $\Delta\delta=-0.86$ ppm, whereas for **1** a shift of only 0.21 ppm results.

Overall, however, the containers exist in *closed* and *open* conformations, and, with varying ease, we can progressively increase the population of the latter forms in their equilibria.

We finally went on to evaluate the key property of our novel container molecules. We added the preferred guest molecules to solutions of **1** and **2** in mesitylene-d_{12} and subjected the resulting encapsulation complexes to the switching stimulus. As shown in Figure 7a, container **1** completely lost its cargo at [CF_3COOD]=2.0 M. Basket **2** behaves essentially identical. The addition of only small amounts of acid is sufficient to release the encapsulated guests because once the H^+ concentration in solution is increased, *open* conformations of **1** and **2** become populated, which are in fast equilibrium with the *closed* forms. As a consequence, the ensemble's constrictive barrier to guest release is completely suspended.

The process is fully reversible: it is illustrated in Figure 7b, how neutralization of the acid with base completely and immediately restores binding within the basket **1**. Again, this observation is identical in the case of **2**. If NEt_3 is used to neutralize the acid CF_3COOD, a room-temperature ionic liquid is formed,[39] which phase separates and can be conveniently removed by syringe. Only the starting encapsulation complex in mesitylene-d_{12} is left and the cycle is completed.

3. Conclusion

In summary, we have reported the synthesis and properties of the novel container molecules **1** and **2**. The molecules completely surround suitable guests within their cavities. The well-defined structures of the baskets lead to strong intrinsic and constrictive binding of smaller molecules with very high selectivity. The selectivity is governed by optimum volume occupancy and the containers can slightly adjust the size of their binding sites to optimize the fraction of filled space. This adaptation is, however, only effective if the volume of the guest does not differ much from optimum. The *closed* conformations of both **1** and **2** are in equilibrium with their respective *open* forms, and the addition of acid leads to population of the latter. The *open* forms have no enforced cavity and instantly release the guest. The process is fully reversible: addition of base completely and immediately restores the guest-hosting properties of the switchable molecular baskets. Enforced inner spaces with switchable portals could assume growing importance for exerting dynamic control over the kinetics of chemical reactions on the inside of molecules. Furthermore, the principle of highly selective hosts, which hold their cargo over long periods of time, and open their stowage in response to a stimulus hold enormous potential in applications such as controlled release of active molecules.

4. Experimental

4.1. Syntheses

Imide **9**, precursor cavitand **5**, and basket **2** were synthesized according to the procedures we have described in the preliminary communication.[17] Cyclobutane was obtained by Wolff–Kishner reduction of cyclobutanone.[40]

4.1.1. General methods

Tetrahydrofuran (THF) and *N*,*N*-dimethylformamide (DMF) were purchased from Fluka ([H_2O] <0.005%). All reactions were carried out under a dry N_2 atmosphere in flame-dried glassware following standard Schlenk techniques. Air was dried by slow passage through 25 cm Blaugel. ^{1}H and ^{13}C NMR spectra were recorded at 298 K on a Bruker ARX 300 or a Bruker Avance DRX 500 spectrometer unless otherwise stated. ^{13}C NMR spectra are ^{1}H broadband decoupled. Chemical shifts δ were referenced to tetramethylsilane (TMS) as an internal standard. High-resolution FT-MALDI ion cyclotron resonance (MALDI-ICR) mass spectra were recorded on a Varian Ion Spec Ultima FT-ICR-MS, with 3-hydroxypyridine-2-carboxylic acid as the matrix. IR spectra were measured of neat samples on a Varian 800 FT-IR spectrometer and absorptions $\tilde{\nu}$ are given, with specification of the intensity as s=strong, m=medium, and w=weak. Melting points were determined on a Büchi B-540 melting point apparatus in open capillary tubes and are uncorrected. Elemental analysis was carried out by the *Mikrolabor* at the Laboratorium für Organische Chemie,

ETH Zürich. Flash chromatography was done as described by Still et al.[41] Medium Pressure Liquid Chromatography (MPLC) was run on a Büchi Sepacore system. Stationary phase for flash chromatography and MPLC was silica gel 60 (Silicycle, 230–400 mesh). Solvents used for MPLC were technical grade and distilled prior to use unless otherwise noted. High-performance gel-permeation chromatography (GPC) was run on a Merck-Hitachi LaChrom D-Line system at 25 °C with UV-detection at 250 nm. HPLC-grade $CHCl_3$ was used as the mobile phase. Stationary phase was a NovoGROM SDV-Gel 100 Å, 10 μm GPC-column of 300×8 mm dimensions; the flow rate was 1 mL/min.

*4.1.2. 2,3-Dichloro-5,7-dioxo-6-(prop-2-inyl)-6,7-dihydro-5H-pyrrolo[3,4-b]pyrazine (**8**)*

5,6-Dichloropyrazine-2,3-dicarboxylic acid anhydride (4360 mg, 19.9 mmol, 1.1 equiv) was suspended in 250 mL THF, propargylic amine was slowly added (997 mg, 1159 μL, 18.1 mmol, 1.0 equiv), and the mixture was heated to gentle reflux for 2.5 h. Then the clear, orange solution was cooled to room temperature, placed in a water bath (≈15 °C), and oxalyl chloride was added dropwise (2642 mg, 1816 μL, 20.8 mmol, 1.2 equiv). Upon the addition of pyridine (4295 mg, 4392 μL, 54.3 mmol, 3.0 equiv), considerable effervescence was observed and a voluminous, cream-colored precipitate appeared. After stirring the mixture for 17 h at room temperature, the dark brown suspension was filtrated through Celite and concentrated to dryness. The residue was taken up with CH_2Cl_2 (300 mL) and a brown solid was removed from the orange-brown solution by filtration. The filtrate was concentrated and the resulting solid remainder was recrystallized from MeOH (170 mL) to give 1855 mg (7.2 mmol, 40%) of a pale golden, flaky, glimmery solid. Mp 229 °C; R_f: 0.40 (CH_2Cl_2); IR: $\tilde{\nu}$ = 785m, 921s, 1012m, 1118s, 1140s, 1162m, 1223m, 1291m, 1311m, 1397m, 1426m, 1482w, 1546w, 1719s, 1736s, 1801w, 2859m, 2934m, 3304s cm^{-1}; ^1H NMR (500 MHz, $CDCl_3$): δ=2.29 (1H, t, J=2.3 Hz), 4.56 (2H, d, J=2.2 Hz) ppm; ^{13}C NMR (75 MHz, $CDCl_3$): δ=27.89, 72.83, 75.71, 143.94, 153.94, 160.81 ppm; HRMS (MALDI-ICR): m/z=255.9679 $[MH]^+$, $C_9H_3N_3O_2Cl_2H^+$ requires 255.9675. Elemental analysis, found: C 42.45, H 1.04, N 16.41; $C_9H_3N_3O_2Cl_2$ requires: C 42.22, H 1.18, N 16.41%.

*4.1.3. (17s,18s,19s,20s)-17,18,19,20-Tetrahexyl-2,4,6,8,10,12,16-octaoxa-3,11(2,3)-diquinoxalina-7,15(2,3)-bis[5,7-dioxo-6-(prop-2-inyl)-6,7-dihydro-5H-pyrrolo[3,4-b]pyrazina]-1,5,9,13(1,2,4,5)-tetrabenzenapentacyclo[11.3.1.$1^{11,5}$.$1^{5,9}$.$1^{9,13}$]icosaphane (**4**)*

r-11,*c*-13,*c*-29,*c*-36-Tetrahexyl-7,10:12,15:24,27:29,32-tetraethano-8,31:14,25-dimethano-11*H*,28*H*-[1,4,14,17]-tetraoxacyclohexacosino[2,3-*b*:15,16*b*′]diquinoxaline-36,38,42,43-tetrol (**7**) (1212 mg, 1.1 mmol, 1 equiv) was dissolved in 60 mL DMF and imide **8** was added (846 mg, 3.4 mmol, 3 equiv). *N*,*N*-Diisopropylethylamine was added dropwise (727 mg, 980 μL, 5.6 mmol, 5 equiv) and the clear yellow solution became green brown within 15 min. After stirring for 17 h at 40 °C, the mixture had become dark black brown and the solvent was removed in vacuo. Purification by MPLC (hexane/EtOAc) gave 969 mg (0.67 mmol, 60%) of a yellow solid. Mp 220 °C; R_f=0.40 (hexane/EtOAc=2:1); GPC: t_R=8.6 min; IR: $\tilde{\nu}$ = 761m, 896m, 935w, 1016w, 1066w, 1118m, 1157m, 1201m, 1230w, 1261w, 1331s, 1369s, 1412m, 1482w, 1735s, 1795w, 2857m, 2927s, 3075w, 3296m cm^{-1}; ^1H NMR (500 MHz, $CDCl_3$): δ=0.87 (12H, m), 1.16–1.46 (32H, m), 1.93 (2H, t, J=2.4 Hz), 2.20 (8H, m), 4.35 (4H, d, J=2.4 Hz), 5.42 (2H, t, J=8.1 Hz), 5.57 (2H, t, J=8.0 Hz), 7.16 (4H, s), 7.47 (4H, m), 7.93 (4H, m), 8.01 (4H, s) ppm; ^{13}C NMR (75 MHz, $CDCl_3$): δ=14.25, 22.85, 27.36, 28.10, 29.51, 29.54, 32.04, 32.06, 32.58, 32.68, 34.50, 34.55, 72.16, 76.73, 118.89, 123.93, 128.59, 129.91, 135.62, 136.87, 139.82, 141.74, 152.19, 152.26, 153.21, 158.51, 161.35 ppm. HRMS (MALDI-ICR): m/z=1443.5901 $[MH]^+$; $C_{86}H_{78}N_{10}O_{12}H^+$ requires 1443.5873.

*4.1.4. (13s,19s,23s,26s)-13,19,23,26-Tetrahexyl-2,11,24,25-octaoxa-16,21(2,3)-diquinoxalina-3,10(2,3)-bis(5,7-dioxo-6,7-dihydro-5H-pyrrolo[3,4-b]pyrazina)-1,12,14,18(1,2,4,5)-tetrabenzenahexacyclo[10.7.3.1^{1,12}.1^{3,18}.1^{10,14}.1^{14,18}]hexacosaphane-5,7-diyne (**1**)*

Precursor cavitand **4** (434 mg, 0.3 mmol, 1 equiv) was dissolved in DMF (150 mL). CuCl (1488 mg, 15 mmol, 50 equiv) was added in one portion, and the solution became brown and cloudy. After addition of $CuCl_2$ (431 mg, 3.0 mmol, 10 equiv), the solution became green and cloudy and air was gently bubbled through for 15 min. The black-green mixture was stirred at room temperature for 16 h and diluted with CH_2Cl_2 (200 mL, 'Baker analyzed' grade). The organic phase was washed with saturated aqueous NH_4Cl solution, until the washing liquors stayed colorless (4×150 mL), with H_2O (150 mL), and saturated aqueous NaCl solution (100 mL). After drying ($MgSO_4$) and concentration in vacuo, a yellow solid remained. This material was purified by flash chromatography (CH_2Cl_2, 'Baker analyzed' grade) to give **1** as a colorless solid (82 mg, 0.06 mmol, 20%), which was dried for 10 days at 10^{-2} mbar (298 K). Mp >248 °C (dec); R_f=0.60 (CH_2Cl_2/MeOH=100:1); t_R (GPC)= 8.7 min; IR: $\tilde{\nu}$ = 637w, 761m, 896w, 1061w, 1157m, 1199m, 1261w, 1329m, 1370s, 1411m, 1481w, 1680w, 1745s, 1792w, 1935w, 2857m, 2927s cm^{-1}; ^1H NMR (500 MHz, $CDCl_3$): δ=0.94 (12H, m), 1.31–1.53 (32H, m), 2.26 (8H, m), 4.44 (4H, s), 5.56 (2H, t, J=8.2 Hz), 5.73 (2H, t, J=8.2 Hz), 7.23 (4H, s), 7.61 (4H, m), 8.15 (4H, m), 8.21 (4H, s) ppm; ^{13}C NMR (75 MHz, $CDCl_3$): δ=14.08, 22.67, 27.62, 27.94, 27.98, 29.33, 29.38, 31.86, 31.91, 32.34, 32.75, 34.10, 34.18, 66.95, 70.79, 119.08, 123.74, 128.76, 129.90, 135.61, 136.92, 139.52, 141.78, 152.02, 152.32, 153.09, 158.62, 160.54 ppm. HRMS (MALDI-ICR): m/z=1441.5743 (M^+); $C_{86}H_{76}N_{10}O_{12}^+$ requires 1441.5717. Elemental analysis, found: C 69.89, H 4.98, N 9.34; $[C_{86}H_{76}N_{10}O_{12}\cdot 0.5CH_2Cl_2]$ requires: C 69.85, H 5.22, N 9.41%.

4.2. NMR experiments

Containers **1** and **2** were directly weighed into new NMR tubes using a Mettler AT-20 balance and dissolved with mesitylene-d_{12} (purchased from ARMAR Chemicals), which had been carefully distilled over a 10 cm *Vigreux* column. Stock solutions of the guests were prepared (2% v/v in distilled mesitylene-d_{12}) and an aliquot was added to the host solutions. Liquid guests were purchased from major suppliers and used without further purification. In the case of cyclobutane stock solutions, their concentration was checked by comparison to a cycloheptane standard before addition to the host. Concentrations of **1** and **2** were ≈3–4 mM and 0.6 equiv of guest was added. ^1H NMR spectra were recorded on a Bruker Avance DRX 500 spectrometer with TMS as an internal standard at 298 K and processed with Bruker TopSpin software.[42] Pulse angle was 30° and acquisition time 5 s. Recording a spectrum of a representative host–guest complex with an additional delay of 10 s between two scans verified that relaxation was complete. The full sequence of Fourier transformation, phase and baseline correction, and integration was repeated at least three times to obtain values for $K_{app}\pm\sigma$. For the determination of thermodynamic parameters, ^1H NMR spectra were recorded at 6–7 temperatures, which were measured with a Greisinger GMH 3710 high-precision thermometer connected to a platinum four-wire temperature sensor embedded in an NMR tube, which was inserted into the probehead instead of the sample. Values for K_{app} were determined for each temperature as described above. All resulting values (at least three for each temperature) were plotted, and van't Hoff analysis gave $\Delta H\pm\sigma$ and $\Delta S\pm\sigma$.

Acknowledgements

This work was supported by the Swiss National Science Foundation (SNF Grant 200020-111533/1 and NCCR 'Nanoscale Science', Basel). We are grateful to B. Brandenberg for acquisition of 2D NMR

data and for technical support, as well as to Dr. C. Thilgen for help with IUPAC nomenclature. We wish to express our sincere gratitude to Prof. Dr. B. Jaun for support and valuable discussions.

Supplementary data

NMR spectra and GPC traces of new compounds, variable temperature NMR spectra, and ROESY data are reproduced in Supplementary data. Furthermore, van't Hoff plots, further description of the spectral changes upon switching, and extensive detail on the molecular dynamics studies and on the cavity size determination are given there. Supplementary data associated with this article can be found in the online version, at doi:10.1016/j.tet.2008.04.102.

References and notes

1. (a) Balzani, V.; Credi, A.; Raymo, F. M.; Stoddart, J. F. *Angew. Chem., Int. Ed.* **2000**, *39*, 3348–3391; (b) Balzani, V.; Credi, A.; Venturi, M. *Molecular Devices and Machines—A Journey into the Nano World*; Wiley-VCH: Weinheim, 2003; (c) Beckman, R.; Beverly, K.; Boukai, A.; Bunimovich, Y.; Choi, J. W.; DeIonno, E.; Green, J.; Johnston-Halperin, E.; Luo, Y.; Sheriff, B.; Stoddart, J. F.; Heath, J. R. *Faraday Discuss.* **2006**, *131*, 9–22; (d) Bonnet, S.; Collin, J.-P.; Koizumi, M.; Mobian, P.; Sauvage, J.-P. *Adv. Mater.* **2006**, *18*, 1239–1250; (e) Feringa, B. L. *J. Org. Chem.* **2007**, *72*, 6635–6652; (f) Kay, E. R.; Leigh, D. A.; Zerbetto, F. *Angew. Chem., Int. Ed.* **2007**, *46*, 72–191.
2. Feynman, R. P. *Eng. Sci.* **1960**, *23*, 22–36.
3. *Molecular Switches*; Feringa, B. L., Ed.; Wiley-VCH: Weinheim, 2001.
4. (a) Rebek, J., Jr.; Trend, J. E.; Wattley, R. V.; Chakravorti, S. *J. Am. Chem. Soc.* **1979**, *101*, 4333–4337; (b) Shinkai, S.; Ogawa, T.; Nakaji, T.; Kusano, Y.; Nanabe, O. *Tetrahedron Lett.* **1979**, *20*, 4569–4572; (c) Shinkai, S.; Nakaji, T.; Ogawa, T.; Shigematsu, K.; Manabe, O. *J. Am. Chem. Soc.* **1981**, *103*, 111–115; (d) Bissell, R. A.; Córdova, E.; Kaifer, A. E.; Stoddart, J. F. *Nature* **1994**, *369*, 133–137; (e) Livoreil, A.; Dietrich-Buchecker, C. O.; Sauvage, J.-P. *J. Am. Chem. Soc.* **1994**, *116*, 9399–9400; (f) Asakawa, M.; Ashton, P. R.; Balzani, V.; Credi, A.; Hamers, C.; Mattersteig, G.; Montalti, M.; Shipway, A. N.; Spencer, N.; Stoddart, J. F.; Tolley, M. S.; Venturi, M.; White, A. J. P.; Williams, D. J. *Angew. Chem., Int. Ed.* **1998**, *37*, 333–337; (g) Kelly, T. R.; De Silva, H.; Silva, R. A. *Nature* **1999**, *401*, 150–152; (h) Koumura, N.; Zijlstra, R. W. J.; van Delden, R. A.; Harada, N.; Feringa, B. L. *Nature* **1999**, *401*, 152–155; (i) *Molecular Catenanes, Rotaxanes and Knots*; Sauvage, J.-P., Dietrich-Buchecker, C., Eds.; Wiley-VCH: Weinheim, 1999; (j) Irie, M. *Chem. Rev.* **2000**, *100*, 1685–1716; (k) Feringa, B. L.; van Delden, R. A.; Koumura, N.; Geertsema, E. M. *Chem. Rev.* **2000**, *100*, 1789–1816; (l) Collier, C. P.; Mattersteig, G.; Wong, E. W.; Luo, Y.; Beverly, K.; Sampaio, J.; Raymo, F. M.; Stoddart, J. F.; Heath, J. R. *Science* **2000**, *289*, 1172–1175; (m) Pease, A. R.; Jeppesen, J. O.; Stoddart, J. F.; Luo, Y.; Collier, C. P.; Heath, J. R. *Acc. Chem. Res.* **2001**, *34*, 433–444; (n) Barboiu, M.; Lehn, J.-M. *Proc. Natl. Acad. Sci. U.S.A.* **2002**, *99*, 5201–5206; (o) Dugave, C.; Demange, L. *Chem. Rev.* **2003**, *103*, 2475–2532; (p) Muraoka, T.; Kinbara, K.; Kobayashi, Y.; Aida, T. *J. Am. Chem. Soc.* **2003**, *125*, 5612–5613; (q) Norikane, Y.; Tamaoki, N. *Org. Lett.* **2004**, *6*, 2595–2598; (r) Leigh, D. A.; Morales, M. Á. F.; Pérez, E. M.; Wong, J. K. Y.; Saiz, C. G.; Slawin, A. M. Z.; Carmichael, A. J.; Haddleton, D. M.; Brouwer, A. M.; Buma, W. J.; Wurpel, G. W. H.; León, S.; Zerbetto, F. *Angew. Chem., Int. Ed.* **2005**, *44*, 3062–3067; (s) Berná, J.; Leigh, D. A.; Lubomska, M.; Mendoza, S. M.; Pérez, E. M.; Rudolf, P.; Teobaldi, G.; Zerbetto, F. *Nat. Mater.* **2005**, *4*, 704–710; (t) Uchida, K.; Izumi, N.; Sukata, S.; Kojima, Y.; Nakamura, S.; Irie, M. *Angew. Chem., Int. Ed.* **2006**, *45*, 6470–6473; (u) Pijper, D.; Feringa, B. L. *Angew. Chem., Int. Ed.* **2007**, *46*, 3693–3696; (v) Dichtel, W. R.; Heath, J. R.; Stoddart, J. F. *Philos. Trans. R. Soc. London, Ser. A* **2007**, *365*, 1607–1625.
5. (a) Hernandez, R.; Tseng, H.-R.; Wong, J. W.; Stoddart, J. F.; Zink, J. I. *J. Am. Chem. Soc.* **2004**, *126*, 3370–3371; (b) Saha, S.; Leung, K. C.-F.; Nguyen, T. D.; Stoddart, J. F.; Zink, J. I. *Adv. Funct. Mater.* **2007**, *17*, 685–693.
6. (a) Moran, J. R.; Karbach, S.; Cram, D. J. *J. Am. Chem. Soc.* **1982**, *104*, 5826–5828; (b) Cram, D. J. *Science* **1983**, *219*, 1177–1183.
7. (a) Moran, J. R.; Ericson, J. L.; Dalcanale, E.; Bryant, J. A.; Knobler, C. B.; Cram, D. J. *J. Am. Chem. Soc.* **1991**, *113*, 5707–5714; (b) Roncucci, P.; Pirondini, L.; Paderni, G.; Massera, C.; Dalcanale, E.; Azov, V. A.; Diederich, F. *Chem.—Eur. J.* **2006**, *12*, 4775–4784.
8. Frei, M.; Marotti, F.; Diederich, F. *Chem. Commun.* **2004**, 1362–1363.
9. (a) Skinner, P. J.; Cheetham, A. G.; Beeby, A.; Gramlich, V.; Diederich, F. *Helv. Chim. Acta* **2001**, *84*, 2146–2153; (b) Azov, V. A.; Jaun, B.; Diederich, F. *Helv. Chim. Acta* **2004**, *87*, 449–462.
10. (a) Azov, V. A.; Schlegel, A.; Diederich, F. *Angew. Chem., Int. Ed.* **2005**, *44*, 4635–4638; (b) Azov, V. A.; Schlegel, A.; Diederich, F. *Bull. Chem. Soc. Jpn.* **2006**, *79*, 1926–1940.
11. (a) Dalcanale, E.; Soncini, P.; Bacchilega, G.; Ugozzoli, F. *J. Chem. Soc., Chem. Commun.* **1989**, 500–502; (b) Soncini, P.; Bonsignore, S.; Dalcanale, E.; Ugozzoli, F. *J. Org. Chem.* **1992**, *57*, 4608–4612; (c) Zampolli, S.; Betti, P.; Elmi, I.; Dalcanale, E. *Chem. Commun.* **2007**, 2790–2792.
12. (a) Hooley, R. J.; Van Anda, H. J.; Rebek, J., Jr. *J. Am. Chem. Soc.* **2006**, *128*, 3894–3895; (b) Purse, B. W.; Rebek, J., Jr. *Proc. Natl. Acad. Sci. U.S.A.* **2006**, *103*, 2530–2534.
13. (a) Gabard, J.; Collet, A. *J. Chem. Soc., Chem. Commun.* **1981**, 1137–1139; (b) Heath, J. R.; O'Brien, S. C.; Zhang, Q.; Liu, Y.; Curl, R. F.; Kroto, H. W.; Tittel, F. K.; Smalley, R. E. *J. Am. Chem. Soc.* **1985**, *107*, 7779–7780; (c) Cram, D. J.; Karbach, S.; Kim, Y. H.; Baczynskyj, L.; Kalleymeyn, G. W. *J. Am. Chem. Soc.* **1985**, *107*, 2575–2576; (d) Tanner, M. E.; Knobler, C. B.; Cram, D. J. *J. Am. Chem. Soc.* **1990**, *112*, 1659–1660; (e) Cram, D. J.; Cram, J. M. *Container Molecules and Their Guests*; Royal Society of Chemistry: Cambridge, 1994; (f) Collet, A. *Comprehensive Supramolecular Chemistry*; Atwood, J. L., Davies, J. E. D., MacNicol, D. D., Vögtle, F., Eds.; Pergamon: Oxford, 1996; Vol. 2, pp 325–365; (g) Jasat, A.; Sherman, J. C. *Chem. Rev.* **1999**, *99*, 931–968; (h) Warmuth, R.; Yoon, J. *Acc. Chem. Res.* **2001**, *34*, 95–105; (i) Turner, D. R.; Pastor, A.; Alajarin, M.; Steed, J. W. *Struct. Bonding* **2004**, *108*, 97–168; (j) Palmer, L. C.; Rebek, J., Jr. *Org. Biomol. Chem.* **2004**, *2*, 3051–3059; (k) Pluth, M. D.; Raymond, K. N. *Chem. Soc. Rev.* **2007**, *36*, 161–171.
14. (a) Wyler, R.; de Mendoza, J.; Rebek, J., Jr. *Angew. Chem., Int. Ed. Engl.* **1993**, *32*, 1699–1701; (b) Branda, N.; Grotzfeld, R. M.; Valdés, C.; Rebek, J., Jr. *J. Am. Chem. Soc.* **1995**, *117*, 85–88; (c) Heinz, T.; Rudkevich, D. M.; Rebek, J., Jr. *Nature* **1998**, *394*, 764–766; (d) Böhmer, V.; Vysotsky, M. O. *Aust. J. Chem.* **2001**, *54*, 671–677; (e) Prins, L. J.; Reinhoudt, D. N.; Timmerman, P. *Angew. Chem., Int. Ed.* **2001**, *40*, 2382–2426; (f) Atwood, J. L.; Barbour, L. J.; Jerga, A. *Proc. Natl. Acad. Sci. U.S.A.* **2002**, *99*, 4837–4841; (g) Ebbing, M. H. K.; Villa, M.-J.; Valpuesta, J.-M.; Prados, P.; de Mendoza, J. *Proc. Natl. Acad. Sci. U.S.A.* **2002**, *99*, 4962–4966; (h) Hof, F.; Craig, S. L.; Nuckolls, C.; Rebek, J., Jr. *Angew. Chem., Int. Ed.* **2002**, *41*, 1488–1508; (i) Rebek, J., Jr. *Angew. Chem., Int. Ed.* **2005**, *44*, 2068–2078; (j) Huerta, E.; Metselaar, G. A.; Fragoso, A.; Santos, E.; Bo, C.; de Mendoza, J. *Angew. Chem., Int. Ed.* **2007**, *46*, 202–205.
15. (a) Fujita, M.; Oguro, D.; Miyazawa, M.; Oka, H.; Yamaguchi, K.; Ogura, K. *Nature* **1995**, *378*, 469–471; (b) Jacopozzi, P.; Dalcanale, E. *Angew. Chem., Int. Ed.* **1997**, *36*, 613–615; (c) Fujita, M. *Chem. Soc. Rev.* **1998**, *27*, 417–425; (d) Saalfrank, R. W.; Uller, E.; Demleitner, B.; Bernt, I. *Struct. Bonding* **2000**, *96*, 149–175; (e) Leininger, S.; Olenyuk, B.; Stang, P. J. *Chem. Rev.* **2000**, *100*, 853–908; (f) Zuccaccia, D.; Pirondini, L.; Pinalli, R.; Dalcanale, E.; Macchioni, A. *J. Am. Chem. Soc.* **2005**, *127*, 7025–7032; (g) Davis, A. V.; Raymond, K. N. *J. Am. Chem. Soc.* **2005**, *127*, 7912–7919; (h) Fiedler, D.; Leung, D. H.; Bergman, R. G.; Raymond, K. N. *Acc. Chem. Res.* **2005**, *38*, 349–358.
16. (a) Barrett, E. S.; Dale, T. J.; Rebek, J., Jr. *J. Am. Chem. Soc.* **2007**, *129*, 8818–8824; (b) Barrett, E. S.; Dale, T. J.; Rebek, J., Jr. *J. Am. Chem. Soc.* **2007**, *129*, 3818–3819.
17. For a communication on some of the properties of **2**, see: Gottschalk, T.; Jaun, B.; Diederich, F. *Angew. Chem., Int. Ed.* **2007**, *46*, 260–264.
18. *MacroModel, version 9.5*; Schrödinger LLC: New York, NY, USA, 2007.
19. (a) Azov, V. A.; Skinner, P. J.; Yamakoshi, Y.; Seiler, P.; Gramlich, V.; Diederich, F. *Helv. Chim. Acta* **2003**, *86*, 3648–3670; (b) Castro, P. P.; Zhao, G.; Masangkay, G. A.; Hernandez, C.; Gutierrez-Tunstad, L. M. *Org. Lett.* **2004**, *6*, 333–336.
20. Cram, D. J.; Choi, H.-J.; Bryant, J. A.; Knobler, C. B. *J. Am. Chem. Soc.* **1992**, *114*, 7748–7765.
21. Wada, M.; Mitsunobu, O. *Tetrahedron Lett.* **1972**, 1279–1282.
22. Körner, S. K.; Tucci, F. C.; Rudkevich, D. M.; Heinz, T.; Rebek, J., Jr. *Chem.—Eur. J.* **2000**, *6*, 187–195.
23. Although bubbling samples of the baskets in mesitylene-d_{12} with argon is effective for qualitative spectral characterization, the method is not useful for quantitative work. The resulting host concentrations were found inaccurate, presumably because droplets of solution were carried off with the gas flow. Therefore, this treatment was not applied in quantitative experiments.
24. The chemical shift of δ=4.3 ppm for CH_2Cl_2 in mesitylene-d_{12} was confirmed in a separate ^{1}H NMR experiment and found identical to literature data for CH_2Cl_2 in benzene-d_6: Gottlieb, H. E.; Kotlyar, V.; Nudelman, A. *J. Org. Chem.* **1997**, *62*, 7512–7515.
25. (a) Craig, S. L.; Lin, S.; Chen, J.; Rebek, J., Jr. *J. Am. Chem. Soc.* **2002**, *124*, 8780–8781; (b) Hooley, R. J.; Van Anda, H. J.; Rebek, J., Jr. *J. Am. Chem. Soc.* **2007**, *129*, 13464–13473.
26. Mecozzi, S.; Rebek, J., Jr. *Chem.—Eur. J.* **1998**, *4*, 1016–1022.
27. (a) Hayashida, O.; Sebo, L.; Rebek, J., Jr. *J. Org. Chem.* **2002**, *67*, 8291–8298; (b) Pirondini, L.; Bonifazi, D.; Cantadori, B.; Braiuca, P.; Campagnolo, M.; De Zorzi, R.; Geremia, S.; Diederich, F.; Dalcanale, E. *Tetrahedron* **2006**, *62*, 2008–2015; (c) Schramm, M. P.; Rebek, J., Jr. *Chem.—Eur. J.* **2006**, *12*, 5924–5933; (d) Ajami, D.; Rebek, J., Jr. *J. Am. Chem. Soc.* **2006**, *128*, 15038–15039; (e) Scarso, A.; Pellizzaro, L.; De Lucchi, O.; Linden, A.; Fabris, F. *Angew. Chem., Int. Ed.* **2007**, *46*, 4972–4975; (f) Rebek, J., Jr. *Chem. Commun.* **2007**, 2777–2789.
28. Zürcher, M.; Gottschalk, T.; Meyer, S.; Bur, D.; Diederich, F. *ChemMedChem* **2007**, *3*, 237–240.
29. (a) Kleywegt, G. J.; Jones, T. A. *Acta Crystallogr., Sect. D* **1994**, *50*, 178–185; (b) Kleywegt, G. J. *Voidoo, version 3.3.3*; Uppsala Software Factory: Uppsala, Sweden, 2007.
30. Bondi, A. *J. Phys. Chem.* **1964**, *68*, 441–451.
31. (a) Jensen, F. R.; Noyce, D. S.; Sederholm, C. H.; Berlin, A. J. *J. Am. Chem. Soc.* **1960**, *82*, 1256–1257; (b) Bovey, F. A.; Hood, F. P., III; Anderson, E. W.; Kornegay, R. L. *J. Chem. Phys.* **1964**, *41*, 2041–2044; (c) Friebolin, H. *Ein- und Zweidimensionale NMR-Spektroskopie: Eine Einführung*, 4th ed.; Wiley-VCH: Weinheim, 2006.
32. O'Leary, B. M.; Grotzfeld, R. M.; Rebek, J., Jr. *J. Am. Chem. Soc.* **1997**, *119*, 11701–11702.
33. Paulini, R.; Müller, K.; Diederich, F. *Angew. Chem., Int. Ed.* **2005**, *44*, 1788–1805.

34. (a) Inoue, Y.; Hakushi, T. *J. Chem. Soc., Perkin Trans. 2* **1985**, 935–946; (b) Dunitz, J. D. *Chem. Biol.* **1995**, *2*, 709–712; (c) Benfield, A. P.; Teresk, M. G.; Plake, H. R.; DeLorbe, J. E.; Millspaugh, L. E.; Martin, S. F. *Angew. Chem., Int. Ed.* **2006**, *45*, 6830–6835; (d) Krishnamurthy, V. M.; Bohall, B. R.; Semetey, V.; Whitesides, G. M. *J. Am. Chem. Soc.* **2006**, *128*, 5802–5812; (e) Starikov, E. B.; Nordén, B. *J. Phys. Chem. B* **2007**, *111*, 14431–14435.
35. (a) Stewart, J. J. P. *J. Mol. Model.* **2007**, *13*, 1173–1213; (b) Stewart, J. J. P. *MOPAC2007, version 7.295L*; Stewart Computational Chemistry: Colorado Springs, CO, USA, 2007.
36. (a) Trembleau, L.; Rebek, J., Jr. *Science* **2003**, *301*, 1219–1220; (b) Scarso, A.; Trembleau, L.; Rebek, J., Jr. *Angew. Chem., Int. Ed.* **2003**, *42*, 5499–5502.
37. For the X-ray crystal structure of a resorcin[4]arene cavitand in the open kite conformation, see Ref. 19a.
38. (a) Bryant, J. A.; Knobler, C. B.; Cram, D. J. *J. Am. Chem. Soc.* **1990**, *112*, 1254–1255; (b) Pirondini, L.; Stendardo, A. G.; Geremia, S.; Campagnolo, M.; Samorì, P.; Rabe, J. P.; Fokkens, R.; Dalcanale, E. *Angew. Chem., Int. Ed.* **2003**, *42*, 1384–1387.
39. Chowdhury, P. K.; Halder, M.; Sanders, L.; Calhoun, T.; Anderson, J. L.; Armstrong, D. W.; Song, X.; Petrich, J. W. *J. Phys. Chem. B* **2004**, *108*, 10245–10255.
40. Roberts, J. D.; Sauer, C. W. *J. Am. Chem. Soc.* **1949**, *71*, 3925–3929.
41. Still, W. C.; Kahn, M.; Mitra, A. *J. Org. Chem.* **1978**, *43*, 2923–2925.
42. *TopSpin, version 2.1*; Bruker BioSpin GmbH: Rheinstetten, Germany, 2007.